

Preparation of $\text{Al}_2\text{O}_3\text{--ZrO}_2$ Ceramics by Infiltration Processing

Dušan Galusek & Ján Majling

Department of Ceramics, Glass and Cement, Slovak Technical University, Radinského 9, SK-81237 Bratislava, Slovak Republic

(Received 17 March 1994; accepted 27 May 1994)

Abstract: Zirconia-toughened alumina was prepared by infiltration of zirconium n-propoxide in n-propanol into the alumina matrix. The precursor was decomposed within the pores of the matrix by *in situ* pyrolysis. Homogeneously distributed zirconia located mainly on the grain surfaces of the alumina grains was observed. Multiple infiltration allowed increase of the zirconia content to 16 wt%. Although unstabilised zirconia was precipitated, in some samples 50% ZrO_2 was present in tetragonal form after the final testing.

INTRODUCTION

Low reliability and fracture toughness of technical ceramics hinder its wider application in industry. Focusing attention on the fabrication of ceramic composites seems to be a promising way of improving their properties. A second, reinforcing phase can be introduced into the matrix phase by different procedures. Infiltration techniques are often used,^{1–10} because they fulfil the necessary condition of composite preparation, i.e. homogeneous distribution of the reinforcing phase. With respect to the proposed application of the composite, the liquid metals,¹ melted inorganic salts^{2–3} or stabilised sols^{5,6} are frequently used for infiltration. Also, a solution of an organic precursor,⁷ or inorganic salt⁸ has been reported.

The possibility of infiltrating the matrix from the surface layer to the whole bulk is one of the additional advantages of this method. In partially infiltrated bodies (infiltration to a certain depth), in the case where the thermal expansion coefficient of the modified layer is lower than the bulk thermal expansion coefficient, the increased toughness is due to compressive stresses introduced into the matrix as a consequence of surface modification, while in fully infiltrated bodies, other toughening mechanisms, such as crack deflection or transformation toughening, are observed. Glass and Green³ and Marple and Green⁴ used partial infil-

tration for the surface modification of the TZP (tetragonal zirconia polycrystals) ceramics by Al_2O_3 ^{2,4} and Al_2O_3 ceramics by SiO_2 ^{5,6,9,10} with the aim of introducing the compressive stresses into the ceramic matrix, and consequently, increasing the strength and fracture toughness of the material.

The bulk of reaction-bonded silicon nitride was modified by Kleber and Weiss.⁷ Infiltration of the Si_3N_4 green samples by siloxane and subsequent pyrolysis produced a residue which changed the pore size distribution, with favourable effects on hardness and Young's modulus of the samples.

Finally, the reasons for using an infiltration procedure for the preparation of ceramic composites can be summarised as follows:

- additional phase can be introduced after the preform was formed by well-established techniques.⁹
- infiltration allows homogeneous distribution of one or more additional phases in the preform.⁹
- variation of infiltration time enables control of the depth of the modified layer.⁹
- additional phase lowers the porosity and subsequently the shrinkage of the preform during sintering.^{3,7}

Despite a relatively large number of papers on the subject of infiltration of ceramic matrices, in-

formation about preparation of the zirconia-reinforced alumina by infiltration technique remains absent. The aim of the present work, therefore, is to prepare $\text{ZrO}_2\text{-Al}_2\text{O}_3$ ceramics by the infiltration technique and to find the optimal processing parameters which secure homogeneous distribution of zirconia within the alumina matrix, as well as the phase composition with a high tetragonal ZrO_2 content.

EXPERIMENTAL

For the fabrication of preforms, three different Al_2O_3 powders were used. Their characteristics are listed in Table 1. Powders were mixed with distilled water with added dispersant. The ammonium salt of the polyacrylic acid SOKRAT 32A, (Chemické závody Sokolov, Czech Republic) was used as a dispersant. The suspension (50 wt% of powder, 1 wt% SOKRAT 32A, 49 wt% water) was ultrasonically treated for 10 min to remove soft agglomerates and evacuated to diminish the amount of entrapped air. The slurry was cast on the plaster of Paris plate into the mould with dimensions $5 \times 5 \times 40$ mm. The preforms obtained were dried and then pre-sintered at different temperatures, from 750 to 1200°C, for one hour, to the strength and porosity which allow manipulation and infiltration, respectively. The temperatures used and the porosity obtained are listed in Table 2.

The density and porosity of the pre-sintered bars was determined using a mercury immersion method, the porosity was measured by mercury porosimetry (Carlo Erba 1520). The solution of zirconium n-propoxide in n-propanol in a weight ratio 70/30, produced by Ventron, Alfa Produkte Karlsruhe, Germany was used for infiltration. The volume fraction of the infiltrant in relation to each particulate sample was calculated with respect to its porosity, i.e. to fill the volume of all open pores with the solution. Zirconium n-propoxide is an extremely moisture-sensitive reagent, therefore all operations were made in a glove box with a dried

Table 2. Temperature of pre-sintering (T) and initial porosity of infiltrated preforms

Material	T [°C]	Porosity [%]
M203	1200	38.0
BCR6	750	50.0
BSM8	800	44.0

air atmosphere. Preforms were dipped in the solution for periods ranging from 24 h to 3 days. Previous unpublished results indicate that 3 day infiltration is long enough for the penetration of the solution into the whole bulk without respect to the porosity of the preform.

After infiltration, the preforms were weighed to determine if all open pores were filled with the solution. The samples were heated at a rate 5°C/min up to 800°C, with one hour duration to decompose the infiltrant and precipitate ZrO_2 . After heating, the weight of the bars was measured again to determine the real ZrO_2 content. To obtain a higher zirconia content, multiple infiltration was used. The samples were then sintered for 3 h at 1550°C and the final density was measured. The phase composition (i.e. tetragonal/monoclinic zirconia ratio with respect to the total amount of zirconia present) both before and after sintering was determined by X-ray powder diffraction analysis. The tetragonal zirconia content was calculated using integral intensities of $(111)_m$, $(\bar{1}\bar{1}1)_m$ and $(101)_t$ peaks.¹¹ The distribution of ZrO_2 in the matrix and the concentration profile of zirconia at the polished cross-section were measured by electron probe microanalyser JEOL JXA 840A. The microstructure of fracture surfaces of sintered samples was observed by scanning electron microscope TESLA BS-300.

Table 1. Properties of Al_2O_3 powders

Material	Used symbol	d_{50} [μm]	Specific area (BET) [$\text{m}^2 \text{g}^{-1}$]	Main impurities
Martoxid ZR-203*	M203	2.8	1–1.5	$\Sigma(\text{Si, Fe, P, Ca}) < 0.2\%$
Baikalox CR6AS2†	BCR6	0.61	9	$\Sigma(\text{Si, Fe, K, Na, Ca}) < 0.1\%$
Baikalox SM8†	BSM8	0.25	10	$\Sigma(\text{Si, Fe, K, Na, Ca}) < 0.1\%$

* Martinswerk GmbH, Berghaim Germany

† Baikowski, France

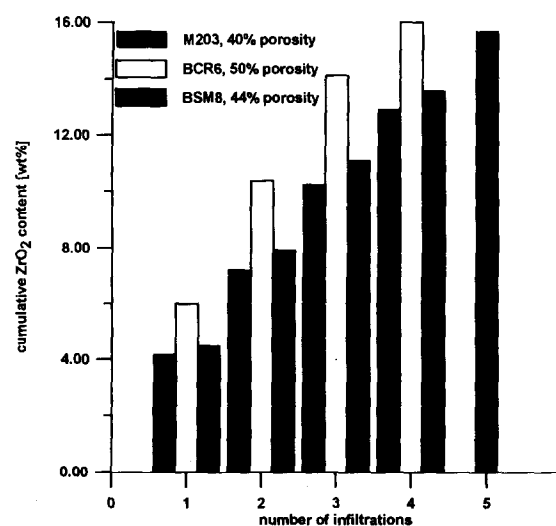


Fig. 1. Cumulative content of ZrO_2 in the Al_2O_3 preforms as a function of the infiltration number.

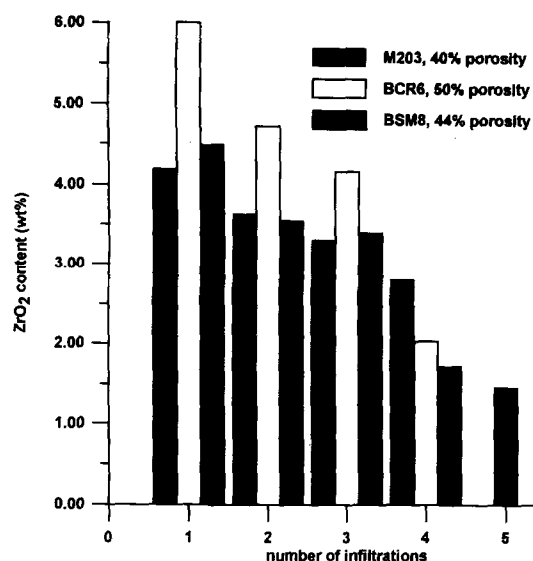


Fig. 2. Content of ZrO_2 introduced into the matrix in single infiltration as a function of the number of infiltrations.

RESULTS AND DISCUSSION

The total weight fraction of zirconia introduced into the preform as a function of the number of infiltrations is shown in Fig. 1. As can be seen from this figure, the content of ZrO_2 introduced into the preform is influenced by the initial porosity of the pre-sintered body. Weight fraction of precipitated ZrO_2 after the first infiltration varies from 4.19 wt% (M203, initial porosity 40 vol%), to 6 wt% (BCR6, 50 vol% initial porosity), as seen from Fig. 1 and Table 2. Figure 2 shows the weight fraction of zirconia precipitated after each infiltration cycle. The weight decrease of ZrO_2 introduced into the matrix is evident. Two explanations of this phenomenon are possible.

(1) Narrow pore channels (open porosity) are gradually closed by the precipitated zirconia. This phenomenon is more pronounced for the preforms with finer microstructure (e.g. BSM8), i.e. with narrow pore channels. As can be seen from Fig. 2, in BSM8 and BCR6 samples, after an initial slow decrease, the amount of zirconia introduced in a single infiltration is strongly decreased after the third infiltration when the total zirconia content reached approximately 8 and 10 wt%, respectively. This can be explained by a closing of the narrow pore channels among the fine grains by precipitated zirconia. More evidence for this explanation is the measurement of the open porosity volume and the pore size distribution measurement performed on BSM8 and BCR6 samples. For example, on BSM8 samples the volume of open pores decreased from $0.139 \text{ cm}^3 \text{ g}^{-1}$ after first infiltration to $0.133 \text{ cm}^3 \text{ g}^{-1}$ after second infiltration. On the other hand, after third infiltration the volume of open pores was only $0.118 \text{ cm}^3 \text{ g}^{-1}$ and remained

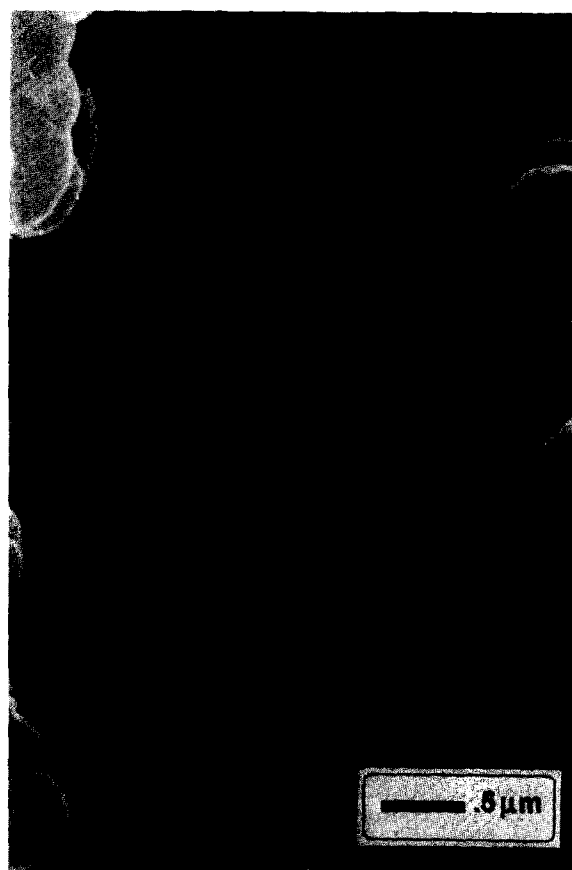


Fig. 3. M203 sample. Precipitated zirconia particles on the surface of the alumina grains.

nearly constant after both the fourth and fifth infiltration (0.114 and $0.112 \text{ cm}^3 \text{ g}^{-1}$, respectively). It is obvious that the pore space accessible to infiltrant was diminished after the third infiltration, i.e. pores under a certain size ($\approx 16 \text{ nm}$) were closed by precipitated zirconia.

On the other hand, M203 powder with mean grain size $2.8 \mu\text{m}$ creates a coarser green microstructure with wider pore channels. As can be seen from Fig. 3, for M203 the introduced amount of zirconia decreased only slightly with a growing infiltration number, i.e. with an increasing fraction of zirconia. Also from Fig. 3, it is obvious that the size of zirconia precipitates is almost negligible with respect to the size of the pores in the body; i.e. the pore channels remain free for liquid penetration and closing of the open pores does not occur.

(2) The amount of zirconia which precipitates within the matrix decreases with the total amount of introduced zirconia, i.e. with an increasing infiltration number. This is probably caused not only by decreasing pore volume, but also by higher evaporation of the infiltrant in the samples with high zirconia content. This situation is shown in Fig. 4. The straight line shows an ideal case, when the real volume fraction of precipitated zirconia is equal to that calculated from the amount of infil-

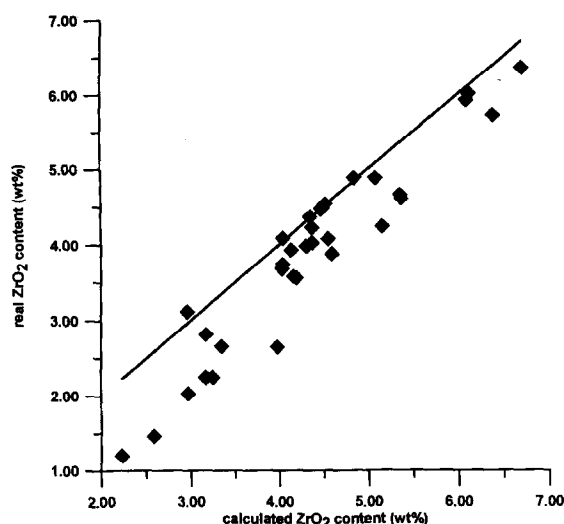


Fig. 4. Deviation between the real content of ZrO_2 in the matrix and the content calculated from the amount of infiltrant.

trant. The points below this line show the real situation. Each point of the diagram represents the weight fraction of precipitated zirconia after a particular infiltration cycle. The diagram is constructed from the measurements performed on all samples under study. As can be seen, especially for low values, which are typical for the infiltration of the preforms with high zirconia content, the actual amount of zirconia is substantially

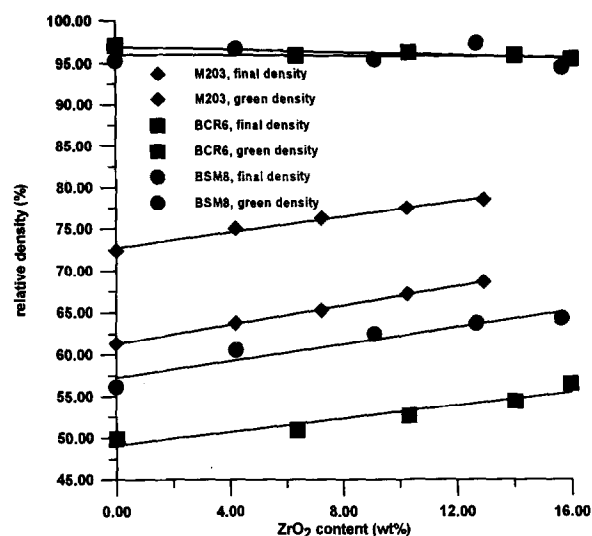


Fig. 5. Green and final density of the infiltrated Al_2O_3 preforms after 3 hours sintering at 1550°C as a function of the ZrO_2 content.

lower than the calculated one. On the other hand, at high values reached by the first and second infiltration, the real situation is close to an ideal case.

Finally, it is possible to conclude, that the decrease of the volume fraction of zirconia after each infiltration cycle is caused by superposition of both previously mentioned mechanisms.

Figure 5 shows the dependence of green density

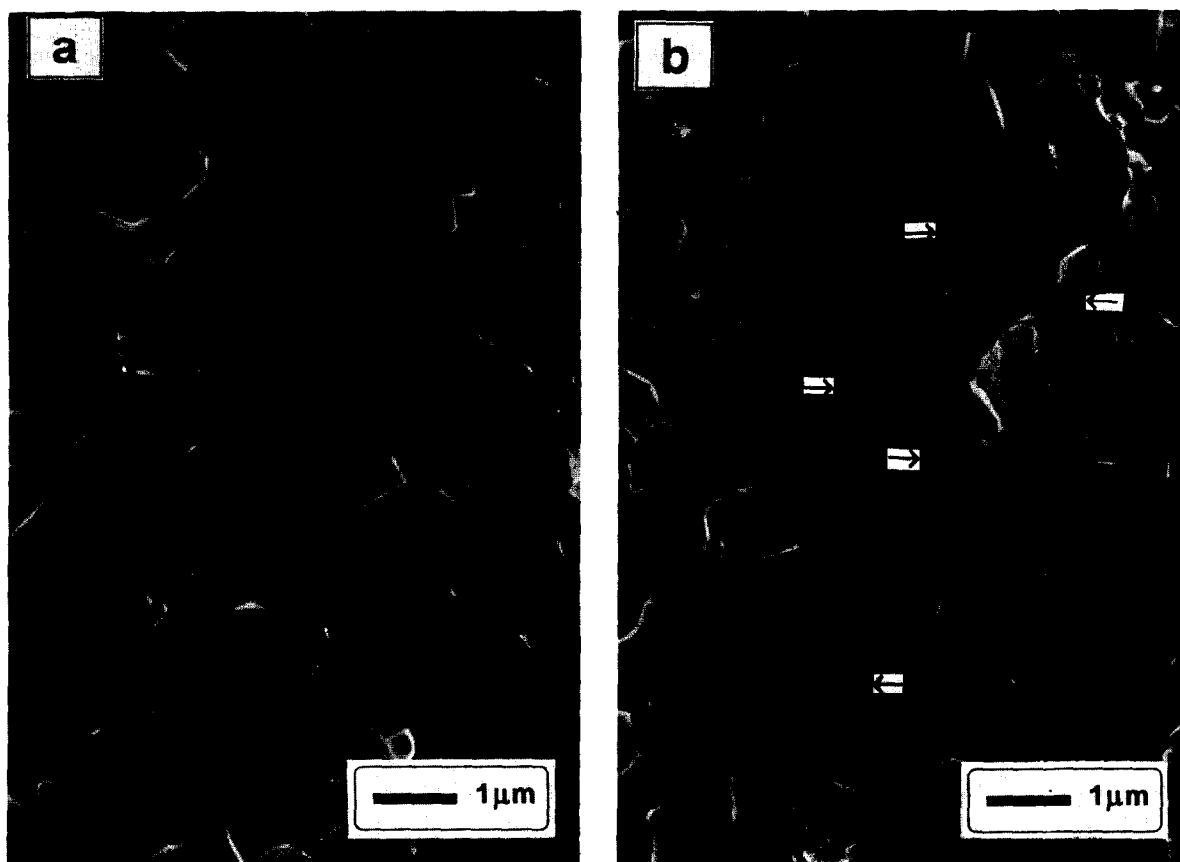


Fig. 6. Microstructures of BSM8 and BCR6 samples after sintering 1550°C , 3 h: (a) BSM8 sample, no zirconia present, (b) BSM8, 9 wt% ZrO_2 , (c) BSM8, 15.7 wt% ZrO_2 , (d) BCR6, no zirconia present, (e) BCR6, 10 wt% ZrO_2 , (f) BCR6, 16.9 wt% ZrO_2 .

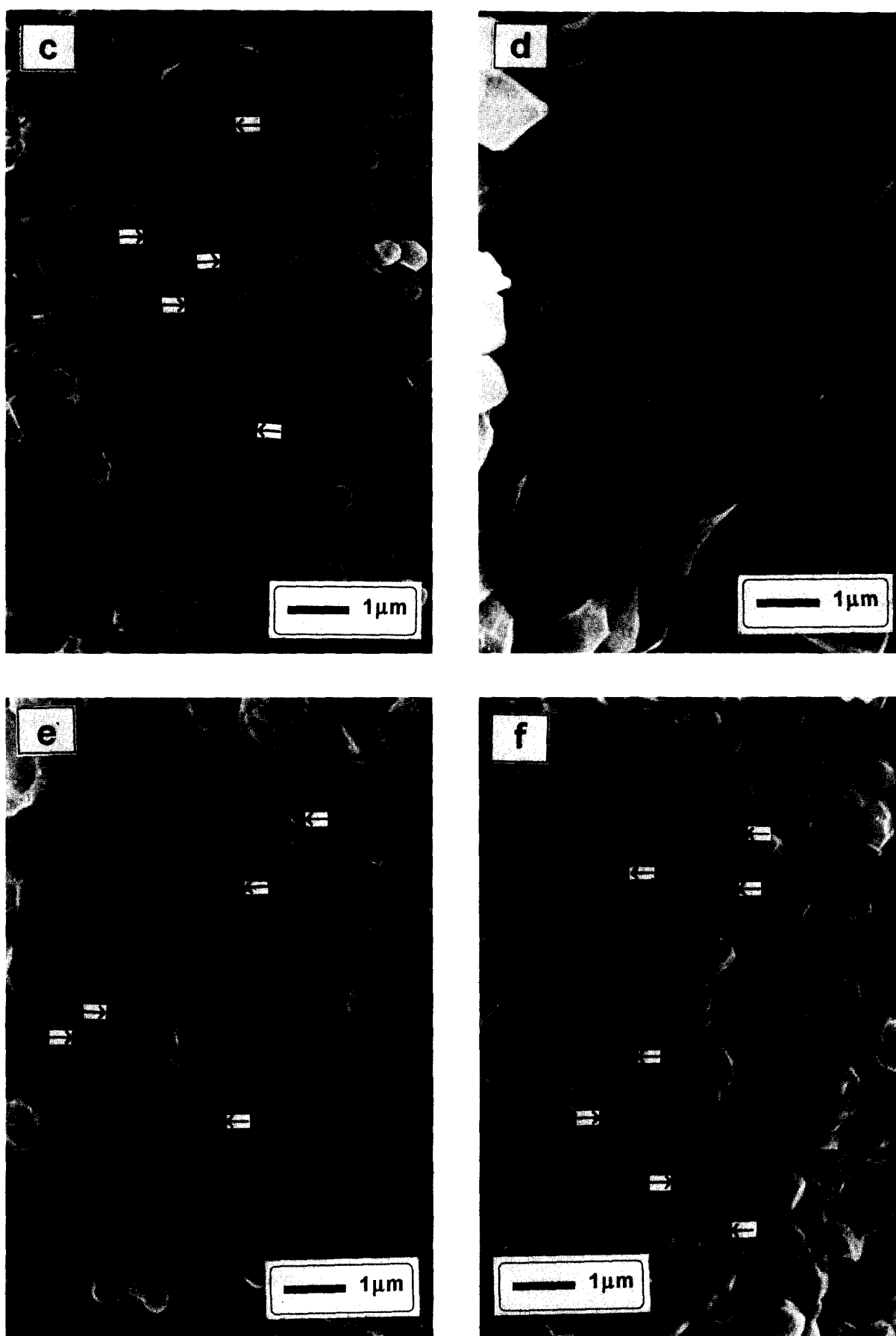


Fig. 6.—Contd.

Table 3. Tetragonal zirconia content in different samples, determined by X-ray diffraction analysis. Tetragonal zirconia content is expressed in vol% of the total ZrO_2 content listed in the second column of the table

Sample name	Total ZrO_2 content [wt%]	t- ZrO_2 content [vol%]	
		before sintering	after sintering
M203-1	12.9	17.3	9.2
M203-2	10.3	18.2	8.3
BCR6-1	16.9	49.3	32.3
BCR6-2	14.0	42.1	10.3
BSM8-1	15.7	54.7	53.2
BSM8-2	12.7	31.4	20.2

of the samples (i.e. the density of the sample after thermal decomposition of the infiltrant) as a function of the zirconia content, as well as the final density of the samples after sintering. Green density grows with increasing zirconia content (for BSM8 sample from 56.0% to 64.2% of theoretical value). Increasing green density obviously results from filling the porosity with zirconia precipitates. On the other hand, maximal density reached by sintering at 1550°C for 3 h does not depend on the weight fraction of zirconia in the alumina matrix. The only exception is the M203 sample, where the final density grows with the increasing volume fraction of zirconia. However, these results are not comparable with BCR6 and BSM8 samples due to the low final density of the M203 sample.

Zirconia creates particles substantially smaller than the crystals of the alumina matrix, located after sintering in the triple points and on grain boundaries of alumina particles. In Fig. 6(b), (c), (e) and (f), the zirconia grains are marked by arrows. It is also obvious from these figures that the size of alumina grains decreases with growing amount of zirconia, i.e. zirconia acts as a grain growth inhibitor in the alumina matrix. In Fig. 6(f) (BSM8 sample with the highest weight fraction of zirconia, 15.7 wt%), the size of marked ZrO_2 grains is about 100–200 nm. According to the literature,¹² this value is low enough to allow the existence of the tetragonal zirconia in the alumina matrix even at room temperature. This is in agreement with the results of the X-ray phase analysis (Table 3), where the highest tetragonal zirconia content was in the samples BSM8 and BCR6 with the highest amount of introduced zirconia. In these samples with the finest microstructures, 50 and 30% of zirconia was present in the tetragonal form after sintering, respectively.

Zirconia concentration line profiles of some selected samples are shown in Fig. 7. Especially in

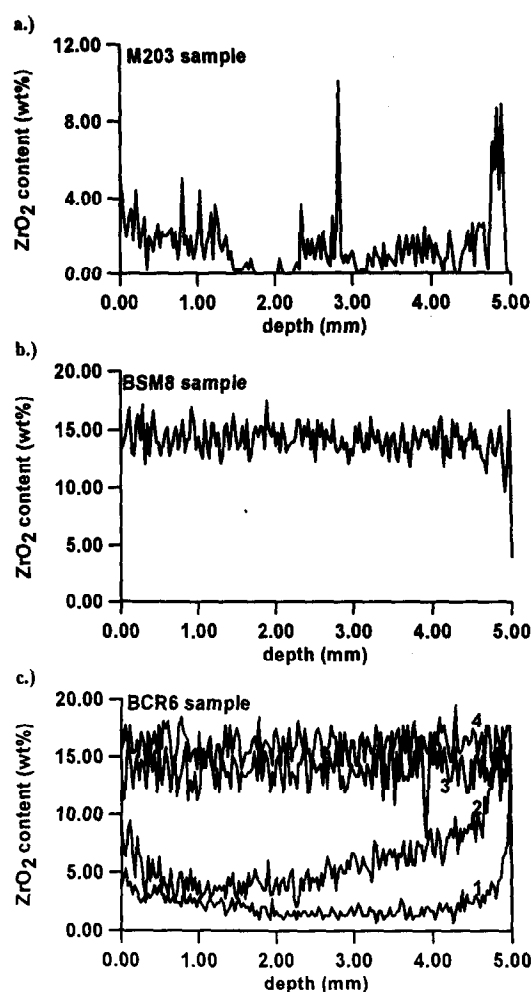


Fig. 7. Concentration line profiles of the ZrO_2 content across the polished sections of the infiltrated samples: (a) M203, (b) BSM8, (c) BCR6 (1—average ZrO_2 content 6 wt%, 2—10.4 wt%, 3—14 wt%, 4—16 wt%).

M203 samples with large particle and pore size, the fluctuation in the ZrO_2 content is considerable. The possible explanation is that some large pores are present (Fig. 3) and precipitated zirconia particles do not fill the voids in the microstructure, but create only a thin layer on the alumina grain surface. On the other hand, in BSM8 and BCR6 samples, the ZrO_2 concentration line profile is nearly constant over the cross-section of samples, especially for higher zirconia contents. In BCR6 samples [Fig. 7(c)] and low zirconia contents (6 and 10.4 wt% of ZrO_2) zirconia concentration near the sample surface is high and decreases with increasing distance from the sample surface. With increasing ZrO_2 content (14, 16 wt%), the concentration of zirconia reached nearly constant value over the measured area.

CONCLUSIONS

1. The infiltration procedure is suitable for preparation of $\text{ZrO}_2\text{--Al}_2\text{O}_3$ composites.

2. Multiple infiltration results in a decrease of the volume fraction of zirconia which precipitates within the matrix after each infiltration cycle. This is due to the superposition of two phenomena:
 - (a) evaporation of the infiltrant during heat treatment.
 - (b) the filling of the pores with precipitated zirconia.
3. Maximal reached density of sintered samples is not influenced by growing zirconia content in the alumina matrix.
4. Infiltration procedure allows a homogeneous distribution of zirconia within the alumina matrix.
5. After the third infiltration, the concentration profile of zirconia reached constant values over the cross-section of the measured sample. Further infiltration allows increase only of the total amount of zirconia in the sample, but causes no change in zirconia distribution in the matrix.

ACKNOWLEDGEMENT

The authors wish to express their thanks to Dr. P. Šajgalík (Slovak Academy of Science, Bratislava) for helpful discussion.

REFERENCES

1. TOY, C. & SCOTT, W., Ceramic-metal composite produced by melt infiltration. *J. Am. Ceram. Soc.*, **73** (1990) 97–101.
2. SÖMIYA, S., (ed.), *Advances in Ceramics, Science and Technology of Zirconia III*, Am. Ceram. Soc., Westerville, OH, 1988, pp. 311–18.
3. MESSING, G. ed., *Ceramic Transactions*, Vol. 1B, Ceramic Powder Science II, Am. Ceram. Soc., Westerville, OH, 1988, pp. 784–91.
4. GLASS, S. J. & GREEN, D. J., Surface Modification of ceramics by partial infiltrations. *Advanced Ceram. Mat.*, **2** (1987) 129–31.
5. MARPLE, B. R. & GREEN, D. J., Mullite/alumina particulate composites by an infiltration technique. *Ceram. Eng. Sci. Proc.*, **10** (1989) 586–7.
6. MARPLE, B. R. & GREEN, D. J., Mullite alumina particulate composites by infiltration processing: II. Infiltration and characterisation. *J. Am. Ceram. Soc.*, **73** (1990) 3611–6.
7. KLEBER, S. & WEISS, H. J., Effect of siloxane infiltration of green samples on properties of RBSN. *J. Eur. Ceram. Soc.*, **10** (1992) 205–11.
8. DUH, J. G. & WAN, J. U., Liquid infiltrations in ZrO_2 ceramics. *J. Mat. Sci. Lett.*, **12** (1993) 473–5.
9. MARPLE, B. R. & GREEN, D. J., Mullite/alumina particulate composites by infiltration processing. *J. Am. Ceram. Soc.*, **72** (1989) 2043–8.
10. MARPLE, B. R. & GREEN, D. J., Incorporation of mullite as a second phase into alumina by an infiltration technique. *J. Am. Ceram. Soc.*, **71** (1988) C431–7.
11. TORAYA, H., YOSHIMURA, M. & SÖMIYA, S., Calibration curve for quantitative analysis of the monoclinic-tetragonal ZrO_2 system by X-ray diffraction. *J. Am. Ceram. Soc.*, **67** (1984) C119–21.
12. HEUER, A. H., ed., *Advances in Ceramics, Science and Technology of Zirconia*, Vol. 3, Am. Ceram. Soc., Columbus, OH, 1981, pp. 137–63.